Quantum Noise Spectroscopy of Dynamical Critical Phenomena

Francisco Machado,[1,2,3] Eugene A. Demler,[4] Norman Y. Yao,[2,3] and Shubhayu Chatterjee[3,5]
[1]ITAMP, Harvard-Smithsonian Center for Astrophysics, Cambridge, Massachusetts 02138, USA
[2]Department of Physics, Harvard University, Cambridge, Massachusetts 02138, USA
[3]Department of Physics, University of California, Berkeley, California 94720, USA
[4]Institute for Theoretical Physics, ETH Zurich, 8093 Zurich, Switzerland
[5]Department of Physics, Carnegie Mellon University, Pittsburgh, Pennsylvania 15213, USA

(Received 28 December 2022; accepted 12 June 2023; published 16 August 2023)

The transition between distinct phases of matter is characterized by the nature of fluctuations near the critical point. We demonstrate that noise spectroscopy can not only diagnose the presence of a phase transition, but can also determine fundamental properties of its criticality. In particular, by analyzing a scaling collapse of the decoherence profile, one can directly extract the critical exponents of the transition and identify its universality class. Our approach naturally captures the presence of conservation laws and distinguishes between classical and quantum phase transitions. In the context of quantum magnetism, our proposal complements existing techniques and provides a novel toolset optimized for interrogating two-dimensional magnetic materials.

DOI: 10.1103/PhysRevLett.131.070801

Continuous phase transitions exhibit remarkable universality across disparate physical systems [1–9]. Owing to the complex interplay between charge, spin, and lattice degrees of freedom, quantum materials have emerged as a particularly fruitful setting for exploring phase transitions [10–13]. To fully characterize such critical phenomena, one must accurately measure both *static* and *dynamical* correlations. The diverging length and time scales at phase transitions require the ability to simultaneously probe low energies and momenta. To obtain such data, one often resorts to one of two broad classes of experimental probes: scattering techniques, where correlations in the material lead to momentum and energy shifts on scattered particles (e.g., neutron scattering, Brillouin light scattering, magnetic optical Kerr, etc.) [14–19]; and magnetic resonance techniques, where fluctuations in the material generate frequency shifts on localized probe spins (e.g., μSR, ESR, NMR, etc.) [20–23].

In this Letter, we propose and analyze noise spectroscopy as a complementary probe of phase transitions and critical phenomena at low frequencies and momenta [Fig. 1(c)]. Our central result is that such spectroscopy enables one to directly characterize the universality class of both classical and quantum phase transitions. In particular, we introduce a simple method to quantitatively extract critical exponents via the scaling collapse of a probe qubit's decoherence profile (i.e., as a function of experimentally tunable control parameters).

We highlight the flexibility and power of this approach in three distinct contexts. First, we discuss how the decoherence profile captures the presence of symmetries and conservation laws. Second, we show that the scaling behavior of the noise near the transition can efficiently characterize both thermal and quantum phase transitions. Finally, we demonstrate how our protocol is able to extract critical exponents—even when the probe qubit is not directly sensitive to the order parameter of the phase transition.

Let us begin by introducing the setup considered throughout this work [Fig. 1(a)]: a single isolated qubit (or a qubit ensemble) is located at a distance d above a sample of interest. The qubit's energy splitting is given by Δ_0 (with quantization axis $\hat{\mathbf{n}}$) and it couples to a time-dependent local field $\mathbf{B}(t)$ with strength γ: $\mathrm{H}(t) = (\Delta_0/2)\hat{\mathbf{n}}\cdot\boldsymbol{\sigma} + [\gamma\mathbf{B}(t)/2]\cdot\boldsymbol{\sigma}$, where σ^α are Pauli operators [26]. While our discussions are applicable to generic qubit platforms (i.e., solid-state spin defects, neutral atoms, trapped ions, superconducting qubits, etc.) coupled to a fluctuating field (i.e., magnetic, electric, strain, etc.), to be specific, we will describe our results in the context of a spin qubit coupled to a fluctuating magnetic field. Three key ingredients relate the properties of the sample to the decoherence dynamics of the probe spin: (i) fluctuations within the material, (ii) the geometry, and (iii) the measurement scheme (i.e., pulse sequence). The fluctuations of the field source O^α within the sample (e.g., current density j^α or spin-density s^α) can be directly characterized by the dynamic structure factor:

$$S^{\alpha\beta}(\mathbf{q},\omega) = \int dt \int d\mathbf{r} e^{i(\omega t - \mathbf{q}\cdot\mathbf{r})}\langle O^\alpha(t,\boldsymbol{r})O^\beta(0,0)\rangle_T, \quad (1)$$

where ω is their frequency, $\mathbf{q}$ their momentum, and $\langle\cdot\rangle_T$ corresponds to the thermal expectation at temperature T.

The relationship between the dynamics of these sources, O^α, and the fluctuating magnetic field at the probe spin location, $\mathbf{B}(t)$, is determined by the system's geometry. This role of geometry is best understood as a *momentum filter function* $W_d^{\alpha\beta}(\hat{\mathbf{n}}, q)$ on the sample's fluctuations. Because $W_d^{\alpha\beta}(\hat{\mathbf{n}}, q)$ is peaked around $q \sim 1/d$, the distance between the qubit and the sample provides direct control of the qubit's sensitivity to the momenta $\mathbf{q}$ of the fluctuations [27]. Simultaneously, different quantization axes $\hat{\mathbf{n}}$ allow one to extract different tensor components of the dynamic structure factor. Akin to geometry, the measurement scheme induces a particular filter function, albeit in frequency space, $W_\tau(\omega)$ [27]. Previous work has focused on T_1-based noise spectroscopy [33–45]; where the qubit is prepared along its quantization axis and its subsequent depolarization dynamics are determined by noise at frequency $\omega = \Delta_0$, leading to a sharp frequency filter function $W_\tau(\omega) \sim \delta(\omega - \Delta_0)$. Given our focus on low frequency behavior, we turn to dephasing-based noise spectroscopy, best exemplified by Ramsey spectroscopy. In this case, the qubit is prepared in a superposition $|\psi\rangle \propto |\uparrow\rangle + |\downarrow\rangle$ along the equator of the Bloch sphere, Fig. 1(b). In each experimental run of duration τ, the magnetic field along the quantization axis, $\hat{\mathbf{n}} \cdot \mathbf{B}(t) = B(t)$, causes the qubit to Larmor precess by an angle $\phi = \gamma \int_0^\tau dt\, B(t)$ [Fig. 1(b)] [46]. Upon averaging over many experimental runs, the resulting density matrix exhibits an off-diagonal term given by $\langle e^{-i2\phi}\rangle \approx e^{-2\langle\phi^2\rangle}$ (which precisely characterizes the qubit's decoherence). If instead a π pulse is applied in the middle of the Larmor precession, the phase accumulated becomes $\phi_{\text{echo}} = \gamma[\int_0^{\tau/2} dtB(t) - \int_{\tau/2}^{\tau} dtB(t)]$, altering the qubit's sensitivity to different frequencies. This effect is precisely captured by the frequency filter function, $W_\tau(\omega)$: for Ramsey spectroscopy, $W_\tau^{(\text{Ramsey})}(\omega) \propto \omega^{-2}\sin^2(\omega\tau/2)$ is peaked around $\omega = 0$ with width $1/\tau$. More intricate pulse sequences, such as spin echo and CPMG, can be used to tailor the properties of the filter function [24,25,27,47].

Bringing all these elements together, the qubit's decoherence profile, $e^{-2\langle\phi^2\rangle}$, depends on the pulse sequence [via $W_\tau(\omega)$], the geometry [via $W_d^{\alpha\beta}(\hat{\mathbf{n}}, q)$] and the properties of the sample of interest [via $S^{\alpha\beta}(q,\omega)$], and can be cast into a simple formula:

$$\langle\phi^2\rangle = \int_{-\infty}^{\infty}\frac{d\omega}{2\pi}W_\tau(\omega)\underbrace{\int_0^\infty\frac{dq}{2\pi}W_d^{\alpha\beta}(\hat{\mathbf{n}},q)S^{\alpha\beta}(q,\omega)}_{\mathcal{N}(\omega)}. \quad (2)$$

Here, $\mathcal{N}(\omega)$ denotes the noise spectral density of the fluctuating magnetic field $B(t)$ generated by the sample.

Thermal phase transitions.—Let us begin by exploring how noise spectroscopy enables the study of thermal (or classical) phase transitions. To be specific, we focus on Ramsey spectroscopy and spin models in two dimensions,

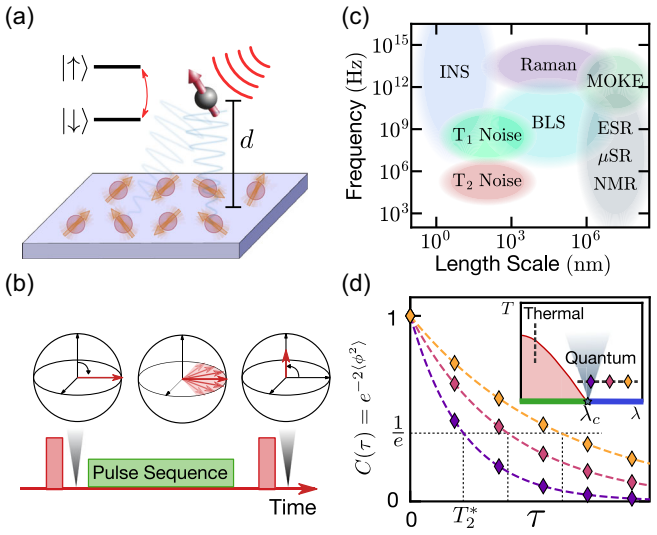

FIG. 1. (a) Schematic of the setup: a two-level probe qubit or qubit ensemble is placed a distance d from a material of interest. Fluctuations in the material generate fluctuating fields at the qubit's location which lead to its decoherence. (b) Using Ramsey spectroscopy or other generalized spin echo pulse sequences [24,25], the qubit's decoherence dynamics can be used to characterize the sample's fluctuations. (c) A summary of the frequency and length scales accessible to different experimental techniques highlights the complementarity of our proposed qubit-based noise spectroscopy (T_2 noise). Techniques depicted include Brillouin light scattering (BLS) [15], magneto-optical Kerr effect (MOKE) [16], Raman spectroscopy [18], inelastic neutron scattering (INS) [17], nuclear magnetic resonance (NMR) [20,21], electron spin resonance [22], and muon spin resonance (μSR) [23]. (d) Schematic of the qubit's decoherence dynamics $C(\tau) = e^{-2\langle\phi^2\rangle}$: as the sample is tuned towards the critical point $\lambda = \lambda_c$ (darker colors, inset), enhanced fluctuations result in a shorter decoherence time T_2^*. More broadly, the decoherence rate and the shape of the profile encode characteristics of the phase transition, including its location, its critical exponents, and the presence of additional symmetries, Fig. 2.

where the momentum filter function takes the form $W_d(\hat{n}, q) \sim q^3 e^{-2qd}$ [27]. First, we consider the classical Ising transition in a two dimensional lattice of spins. Although we are ultimately interested in the structure factor $S^{\alpha\beta}(\mathbf{q},\omega)$ close to the transition, it is more convenient to analyze the behavior of the dynamical susceptibility $\chi^{\alpha\beta}(\mathbf{q},\omega)$. Fortunately, the two are intimately connected via the fluctuation-dissipation theorem: $S^{\alpha\beta}(\mathbf{q},\omega) = (2T/\omega)\times \text{Im}[\chi^{\alpha\beta}(\mathbf{q},\omega)]$. We focus on $\alpha = \beta = z$ as it captures the critical correlations of the Ising order parameter—the coarse-grained magnetization density. To understand the fluctuations of the order parameter, we need to consider the slow relaxation dynamics toward equilibrium. These dynamics are dominated by long-wavelength fluctuations, and can be accounted for by a simple phenomenological model, $\chi^{-1}(\omega,\mathbf{q}) = \chi^{-1}(\mathbf{q}) - [i\omega/\Gamma(\mathbf{q})]$ [2,9,49–51], where $\Gamma(\mathbf{q})$ is the relaxation rate of the $\mathbf{q}$-Fourier mode.

As one approaches the critical temperature T_c, the order-parameter correlation length ξ diverges as $|T - T_c|^{-\nu}$; within mean-field theory $\nu = 1/2$ and $S^{zz}(\mathbf{q}, \omega)$ becomes

$$S^{zz}(\mathbf{q}, \omega) = \frac{2T\Gamma(\mathbf{q})}{\Gamma(\mathbf{q})^2 J^2 (\xi^{-2} + q^2)^2 + \omega^2}. \tag{3}$$

As perhaps expected, independent of the details of $\Gamma(\mathbf{q})$, the magnetic field noise exhibits critical enhancement as one approaches the transition—$S^{zz}(\mathbf{q}, \omega)$ monotonically increases as the correlation length diverges and the minimum of the decoherence time T_2^* diagnoses the critical temperature [Fig. 2(a)].

Crucially, noise spectroscopy enables the direct and quantitative characterization of critical phenomena, making it particularly amenable for studying transitions that deviate from the mean-field expectation. More specifically, scaling considerations enable the derivation of an expression for $\langle \phi^2 \rangle$:

$$\langle \phi^2 \rangle = \frac{T\tau}{d^{2+\eta-z}} F\left(\frac{\tau}{d^z}, \frac{d}{\xi}\right), \qquad \xi \propto |T - T_c|^{-\nu}, \tag{4}$$

where η is the anomalous scaling exponent, z is the dynamical exponent, and the scaling function F depends on details of the dynamics. By varying the distance d, the time τ, and the temperature T [Fig. 2(c)], one can obtain a two-parameter scaling collapse for $\langle \phi^2 \rangle$ which immediately determines the critical exponents [Fig. 2(d)].

Symmetries and conservation laws.—In addition to extracting critical exponents, certain qualitative features of the transition can be obtained from the scaling behavior of $\langle \phi^2 \rangle$ with τ. As an example, we demonstrate how our approach naturally distinguishes between transitions with and without order-parameter conservation; for concreteness, let us return to the 2D classical Ising transition within mean-field theory.

We begin by focusing on the late-time decoherence dynamics, $\omega_0 \tau \gg 1$, where ω_0 is the width of the noise spectral density $\mathcal{N}(\omega)$ [Eq. (2)] [27]. When the order parameter (i.e., the $\mathbf{q} = 0$ spin component) is not conserved, its decay rate $\Gamma(\mathbf{q} = 0)$ will be a nonzero constant Γ_0, leading to a dynamical exponent $z = 2$ [52]. As shown in Fig. 2(b), this implies that $\langle \phi^2 \rangle$ exhibits an (almost) linear scaling with τ (see Table I). In contrast, when the order parameter is conserved, its decay rate $\Gamma(\mathbf{q} = 0)$ must vanish. As a result, the small $\mathbf{q}$ behavior of $\Gamma(\mathbf{q})$ is quadratic, $\Gamma(\mathbf{q}) \sim \sigma_s \mathbf{q}^2$, corresponding to diffusive spin correlations away from criticality. However, at criticality, the correlation length ξ diverges and the spin-diffusion constant $D_s = \sigma_s \xi^{-2}$ goes to zero, leading to a dynamical exponent $z = 4$ as per Eq. (3). Crucially, this results in a nonanalytic behavior of the noise-spectral density $\mathcal{N}(\omega) \sim 1/\sqrt{\omega}$ at low frequencies, manifesting itself as a different late-time scaling, $\langle \phi^2 \rangle \sim \tau^{3/2}$ [Fig. 2(b) and Table I].

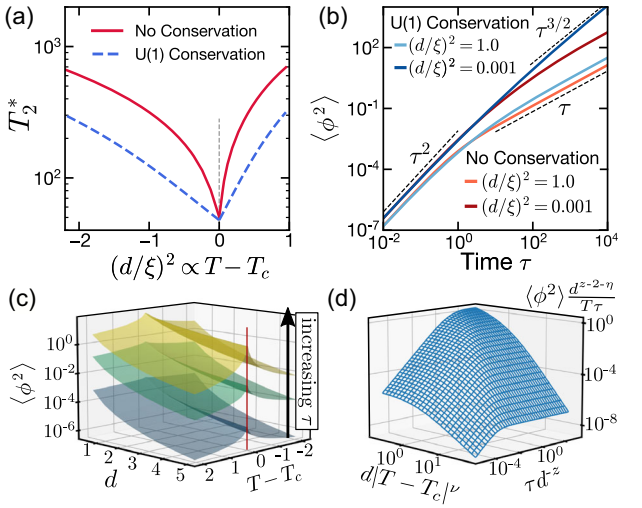

FIG. 2. (a) Behavior of the Ramsey decoherence time, T_2^*, across a phase transition. T_2^* exhibits a sharp feature at the transition, whose details are determined by the presence (or absence) of a conservation law in the order parameter. (b) Decoherence dynamics in the presence of different symmetries (with or without a conserved order parameter) and near or far from criticality [$(d/\xi)^2 = 0.001$ and $(d/\xi)^2 = 1$]. The presence of the conservation law modifies the late-time behavior of $\langle \phi^2 \rangle$—from $\tau \log \tau$ to $\tau^{3/2}$. (c) Decoherence dynamics as a function of the distance to sample d and temperature T for different times τ. $\langle \phi^2 \rangle$ is computed for Ramsey spectroscopy in the case of a classical Ising phase transition with no conservation law. (d) By performing a scaling collapse of $\langle \phi^2 \rangle(d, \tau, T)$, one can directly extract the critical exponents of the transition.

A few remarks are in order. First, at short times, $\omega_0 \tau \ll 1$, the material dynamics are essentially "frozen" and the qubit is only sensitive to the static components of the noise, leading to $\langle \phi^2 \rangle \sim \tau^2$. A complementary perspective is that the Ramsey filter function is significantly broader than the noise spectral density and the probe integrates the response across all frequencies. The location of the crossover between this early-time behavior and the late-time dynamics [Fig. 2(b)] provides a direct measurement of the correlation time associated with the material's intrinsic dynamics [53,54]. Second, the scaling of the qubit's decoherence time with distance d also provides insight into the approach to criticality. In particular, within the critical regime, $d \ll \xi$, the qubit's decoherence will be relatively insensitive to the sample-probe distance. In the opposite limit, $d \gg \xi$, the qubit's decoherence exhibits a significantly stronger *power-law* dependence on d (see Table I).

Quantum phase transitions.—Let us now turn our attention to quantum phase transitions, where the ground state exhibits an abrupt, qualitative change upon tuning some parameter λ (e.g., pressure, electron density, etc.). The key distinction from the thermal case is the sensitivity of the qubit's decoherence to the spectral gap Δ, which goes to

TABLE I. Critical and noncritical scaling of $\langle\phi^2\rangle$ for paradigmatic models of classical and quantum phase transitions [2] with temperature T, distance d, and time τ, in the limit $\omega_0\tau \gg 1$. The scaling behavior of $\langle\phi^2\rangle$ for the thermal phase transitions is presented within mean-field theory, where $\eta = 0$. For quantum transitions away from criticality ($T \ll \delta$), we do not include prefactors of T (since the noise is dominated by the exponential $e^{-\delta/T}$) [27].

Nature of transition	Phase transition	Paradigmatic model	Conserved Quantity	Accessible critical exponents	Noise $\langle\phi^2\rangle$ at criticality	Noise $\langle\phi^2\rangle$ away from criticality
Thermal	Paramagnet to Ferromagnet	Ising	N/A	ν, η, z	$(T\tau/\Gamma_0)\ln(\tau\Gamma_0/d^2)$	$(T\tau\xi^4/\Gamma_0 d^4)$
		XXZ	S^z	ν, η, z	$(T\tau^{3/2}/\sqrt{\sigma_s})$	$(T\tau\xi^4/\sigma_s d^2)$
Quantum	Para to Ferro	Ising	N/A	η, ν, z	$T^{(2+\eta)/z}\tau\ln(c/dT^{1/z})$	$(\tau/d^4)e^{-a_2\delta/T}$
	Para to AFM	Heisenberg	**S**	$z\nu$	$(T^3\tau/d^2)$	$(\tau/d^2)e^{-a_3\delta/T}$

zero at the quantum critical point, $\lambda = \lambda_c$. As a result, $\langle\phi^2\rangle$ still exhibits a simple scaling function Ψ, albeit with an additional scaling parameter Δ/T:

$$\langle\phi^2\rangle = T^{\frac{2+\eta-z}{z}}\Psi\left(\Delta\tau, \Delta d^{1/z}, \frac{\Delta}{T}\right), \qquad \Delta \propto |\lambda - \lambda_c|^{z\nu}. \quad (5)$$

In direct analogy to the thermal case, the critical exponents can be extracted via a scaling data collapse of the decoherence as a function of any three of the four parameters: (i) temperature T, (ii) tuning parameter λ, (iii) sample-probe distance d, and (iv) time τ.

Despite their similarities, the quantum and thermal phase transitions are distinguishable by the *temperature* scaling of $\langle\phi^2\rangle$. Away from criticality ($\Delta/T \gg 1$), the noise is controlled by thermally activated excitations on top of the ground state and is exponentially suppressed in Δ/T leading to $\langle\phi^2\rangle \sim e^{-a\Delta/T}$ for $a > 0$. Near the critical point ($\Delta/T \to 0$), Ψ approaches a constant and thus $\langle\phi^2\rangle$ scales as a power law in temperature. By contrast, in classical phase transitions, the noise will always exhibit power-law correlations with temperature (see Table I).

The ability for noise spectroscopy to probe quantum phase transitions is extremely generic—the qubit does not need to couple to the order parameter, nor does the ordered phase need to be gapped. We highlight this flexibility by studying the noise spectroscopy of a different transition, namely, the continuous symmetry breaking transition between a quantum paramagnet and a collinear Néel antiferromagnet in the two-dimensional Heisenberg model [5,55–59]. The order parameter for this transition is the staggered magnetization density which oscillates at the lattice scale; since this length scale is significantly smaller than the sample-probe distance d, the qubit is insensitive to fluctuations of the order parameter. Rather, its decoherence is determined by the long-wavelength fluctuations of the spin density, which remain conserved owing to the Hamiltonian's SO(3) spin-rotation symmetry. Consequently, the dynamic structure factor takes a simple diffusive form $S^{zz}(\mathbf{q},\omega) = [2T\chi_u D_s\mathbf{q}^2/\omega^2 + (D_s\mathbf{q}^2)^2]$ [analogous to Eq. (3)] with diffusion constant D_s and uniform static susceptibility χ_u; at late times, the decoherence dynamics take on a simple form $\langle\phi^2\rangle \propto (T\tau/d^2)(\chi_u/D_s)$ that depends only on the ratio (χ_u/D_s). The key ingredient that determines both χ_u and D_s on either side of this quantum transition is an intrinsic energy scale δ—in the antiferromagnet $\delta = \rho_s$ is the spin stiffness associated with creating spatially nonuniform textures of the order parameter, while in the paramagnet $\delta = \Delta$ is simply the spectral gap. Specifically, in the vicinity of the transition, both D_s and χ_u are universal functions of the ratio between the energy scale δ and temperature T, and thus the decoherence is controlled by δ/T [5,58,59].

We are now in a position to understand how noise spectroscopy can characterize this transition. First, let us focus on the regime away from criticality ($T \ll \delta$). In this case, decoherence becomes suppressed with temperature owing to a divergent diffusion coefficient $D_s \sim e^{\delta/T}$ and a nondivergent susceptibility χ_u [27]. By fixing T and τ and varying λ, the combined critical exponents $z\nu$ can be extracted from the stretched exponential decay of $\langle\phi^2\rangle \sim (\tau/d^2)e^{-a_3|\lambda-\lambda_c|^{z\nu}/T}$. On the other hand, in the quantum critical regime ($T \gg \delta$ and $\lambda \sim \lambda_c$), temperature is the only relevant energy-scale that determines both χ_u and D_s, and thus, the scaling of the decoherence is simply a power-law in temperature, $\langle\phi^2\rangle \sim T^3$ [27]. This provides a clear, quantitative signature that the system is in the critical regime.

A few remarks are in order. First, the detection of critical exponents in the absence of direct coupling between the qubit and the order parameter can also be applied to thermal phase transitions. Second, given the sensitivity of the low-energy physics to underlying symmetries, the ability to carefully probe such dynamics could enable the diagnosis of symmetry-breaking interactions. Third, we have thus far, restricted our analysis to Gaussian noise, where two-point correlations are sufficient to fully describe the probe qubit's decoherence. The presence of higher-order moments in the noise distribution can affect the dynamics, especially near the transition, where $\xi \gtrsim d$. Interestingly, one can obtain the

corresponding scaling forms and isolate these non-Gaussian contributions via pulse-sequence engineering [27,60–62]. Finally, for some materials, the surface and bulk degrees of freedom can exhibit distinct critical phenomena, altering the probe qubit's decoherence dynamics [63–65]. In this context, the sample-probe distance determines the relative contributions of surface and bulk fluctuations to the qubit's decoherence and can be used to isolate and characterize each transition separately. However, to quantitatively characterize both critical phenomena, a more nuanced scaling theory is required.

Experimental blueprint.—Our protocol can be applied to investigate a variety of critical phenomena, ranging from ferroelectric ordering [43,66] and structural phase transitions [65,67–69], to magnetic ordering [70–72] and superconductivity [40,41,73,74]. In what follows, we highlight our approach in the context of magnetic insulators probed via solid-state, electronic spin defects. We focus on two particular defects—the negatively charged boron vacancy (V_B^-) in hexagonal boron nitride (hBN) [75–78] and the nitrogen-vacancy (NV) color center in diamond [79–81]—with the goal of highlighting their complementary operating modalities. The former can be created within flakes of hBN that are directly placed on a sample of interest [77], while the latter can be embedded within the tip of a (diamond) cantilever and used as a scanning probe [82–85]. Both defects feature spin $S = 1$ electronic ground states with zero-field splittings in the ∼GHz regime [Fig. 1(c)]. Two spin states (forming our probe qubit) can be isolated by either resolving the hyperfine interaction or via an external magnetic field. The frequency range of T_2-based noise spectroscopy, ∼kHz–MHz, is limited by the defect's local environment and the achievable Rabi frequency for pulsed control [86–90].

Both NV centers and V_B^- defects are particularly well placed for studying two-dimensional magnetic materials. As an example, consider monolayer CrI_3, a two-dimensional magnet with an Ising transition at $T_c \approx 45$ K [91–95]. We estimate that in the diffusive regime, the sampled-induced decoherence time will be approximately, $T_2^{\text{echo}} \approx 5$ μs (using $T \approx 60$ K and $d = 10$ nm) [27], with critical fluctuations near the transition further reducing this value [96]. Crucially, this additional noise dominates over the NV's intrinsic decoherence, $T_2^{\text{echo}} \sim 100$ μs [90,98], enabling its detection. Zooming out, the broader landscape of van der Waals heterostructures and moiré materials offers a wide range of correlated insulators and magnetic transitions to explore [99,100]. For example, pressure-driven quantum critical points in two dimensional materials, such as FeSe [101,102], as well as strain-tuned magnetic transitions in monolayer metallic halides, such as the aforementioned CrI_3 [103], can be accessed by directly incorporating the NV center into diamond anvil cells [65,73,104], while magnetic domain formation can be imaged *in situ* by directly incorporating V_B^- into the hBN that encapsulates many 2D materials [105,106]. Simultaneously, the detection and characterization of spin and charge fluctuations can elucidate the nature of the magnetic order in twisted bilayer graphene [107–113], as well as shed light into the continuous Mott transition recently observed in moiré transition metal dichalcogenides [100,114,115].

We gratefully acknowledge discussions with and the insights of K. Akkaravarawong, E. Davis, Z. Dai, S. Hsieh, J. R. Nieva, S. Whitsitt, M. P. Zaletel, and C. Zu. This work was supported in part by the U.S. Department of Energy through BES (Grant No. DE-SC0019241) and through the Materials Sciences and Engineering Division (Contract No. DE-AC02-05-CH11231), the AFOSR through the MURI program (Grant No. W911NF-20-1-0136), the David and Lucile Packard Foundation, the Alfred P. Sloan foundation. F. M. acknowledges support from the NSF through a grant for ITAMP at Harvard University. E. D. acknowledges support from the Swiss National Science Foundation under Division II.

[1] L. D. Landau and E. M. Lifshitz, *Statistical Physics: Volume 5* (Elsevier, New York, 2013), Vol. 5.
[2] J. Cardy, *Scaling and Renormalization in Statistical Physics* (Cambridge University Press, Cambridge, England, 1996), Vol. 5.
[3] N. Goldenfeld, *Lectures on Phase Transitions and the Renormalization Group* (CRC Press, Boca Raton, 1992).
[4] P. Coleman, *Introduction to Many-Body Physics* (Cambridge University Press, Cambridge, England, 2015).
[5] S. Sachdev, Handbook of Magnetism and Advanced Magnetic Materials (2007), 10.1002/9780470022184.hmm108.
[6] S. L. Sondhi, S. M. Girvin, J. P. Carini, and D. Shahar, Rev. Mod. Phys. **69**, 315 (1997).
[7] T. Vojta, Ann. Phys. (N.Y.) **9**, 403 (2000).
[8] M. Vojta, Rep. Prog. Phys. **66**, 2069 (2003).
[9] P. C. Hohenberg and B. I. Halperin, Rev. Mod. Phys. **49**, 435 (1977).
[10] B. Keimer and J. Moore, Nat. Phys. **13**, 1045 (2017).
[11] D. Basov, R. Averitt, and D. Hsieh, Nat. Mater. **16**, 1077 (2017).
[12] W. Li, X. Qian, and J. Li, Nat. Rev. Mater. **6**, 829 (2021).
[13] F. Giustino, J. H. Lee, F. Trier, M. Bibes, S. M. Winter, R. Valentí, Y.-W. Son, L. Taillefer, C. Heil, A. I. Figueroa *et al.*, J. Math. Phys. (N.Y.) **3**, 042006 (2021).
[14] L. Van Hove, Phys. Rev. **95**, 1374 (1954).
[15] F. Kargar and A. A. Balandin, Nat. Photonics **15**, 720 (2021).
[16] T. Haider, Int. J. Electromagn. Appl **7**, 17 (2017).
[17] D. L. Price and F. Fernandez-Alonso, in *Experimental Methods in the Physical Sciences* (Elsevier, New York, 2013), Vol. 44, pp. 1–136.
[18] *Raman Spectroscopy of Two-Dimensional Materials*, edited by P.-H. Tan, Springer Series in Materials Science Vol. 276 (Springer, New York, 2019), ISBN 9789811318276 9789811318283.

[19] T. X. Zhou, J. J. Carmiggelt, L. M. Gächter, I. Esterlis, D. Sels, R. J. Stöhr, C. Du, D. Fernandez, J. F. Rodriguez-Nieva, F. Büttner *et al.*, Proc. Natl. Acad. Sci. U.S.A. **118**, e2019473118 (2021).

[20] P. J. Hore, *Nuclear Magnetic Resonance* (Oxford University Press, USA, 2015).

[21] C. Berthier, M. Horvatić, M.-H. Julien, H. Mayaffre, and S. Krämer, C.R. Phys. **18**, 331 (2017).

[22] K. Katsumata, J. Phys. Condens. Matter **12**, R589 (2000).

[23] A. D. Hillier, S. J. Blundell, I. McKenzie, I. Umegaki, L. Shu, J. A. Wright, T. Prokscha, F. Bert, K. Shimomura, A. Berlie *et al.*, Nat. Rev. Methods Primers **2**, 1 (2022).

[24] L. M. K. Vandersypen and I. L. Chuang, Rev. Mod. Phys. **76**, 1037 (2005).

[25] J. Choi, H. Zhou, H. S. Knowles, R. Landig, S. Choi, and M. D. Lukin, Phys. Rev. X **10**, 031002 (2020).

[26] Throughout this work we use the natural unit convention where $k_b = \hbar = 1$.

[27] See Supplemental Material at http://link.aps.org/supplemental/10.1103/PhysRevLett.131.070801 for more details, which includes Refs. [28–32].

[28] J. Choi, H. Zhou, H. S. Knowles, R. Landig, S. Choi, and M. D. Lukin, Phys. Rev. X **10**, 031002 (2020).

[29] H. Zhou, J. Choi, S. Choi, R. Landig, A. M. Douglas, J. Isoya, F. Jelezko, S. Onoda, H. Sumiya, P. Cappellaro *et al.*, Phys. Rev. X **10**, 031003 (2020).

[30] C. J. Chen, *Introduction to Scanning Tunneling Microscopy Third Edition*, Monographs on the Physics and Chemistry of Materials (Oxford University Press, Oxford, New York, 2021), third edition, new to this edition, ISBN 978-0-19-885655-9.

[31] J. A. Sobota, Y. He, and Z.-X. Shen, Rev. Mod. Phys. **93**, 025006 (2021).

[32] S. Sachdev, Nucl. Phys. **B464**, 576 (1996).

[33] S. Kolkowitz, A. Safira, A. High, R. Devlin, S. Choi, Q. Unterreithmeier, D. Patterson, A. Zibrov, V. Manucharyan, H. Park *et al.*, Science **347**, 1129 (2015).

[34] K. Agarwal, R. Schmidt, B. Halperin, V. Oganesyan, G. Zaránd, M. D. Lukin, and E. Demler, Phys. Rev. B **95**, 155107 (2017).

[35] J. F. Rodriguez-Nieva, K. Agarwal, T. Giamarchi, B. I. Halperin, M. D. Lukin, and E. Demler, Phys. Rev. B **98**, 195433 (2018).

[36] B. Flebus and Y. Tserkovnyak, Phys. Rev. Lett. **121**, 187204 (2018).

[37] S. Chatterjee, J. F. Rodriguez-Nieva, and E. Demler, Phys. Rev. B **99**, 104425 (2019).

[38] A. Rustagi, I. Bertelli, T. van der Sar, and P. Upadhyaya, Phys. Rev. B **102**, 220403(R) (2020).

[39] H. Wang, S. Zhang, N. J. McLaughlin, B. Flebus, M. Huang, Y. Xiao, E. E. Fullerton, Y. Tserkovnyak, and C. R. Du, Sci. Adv. **6**, eabg8562 (2022).

[40] S. Chatterjee, P. E. Dolgirev, I. Esterlis, A. A. Zibrov, M. D. Lukin, N. Y. Yao, and E. Demler, Phys. Rev. Res. **4**, L012001 (2022).

[41] P. E. Dolgirev, S. Chatterjee, I. Esterlis, A. A. Zibrov, M. D. Lukin, N. Y. Yao, and E. Demler, Phys. Rev. B **105**, 024507 (2022).

[42] T. I. Andersen, B. L. Dwyer, J. D. Sanchez-Yamagishi, J. F. Rodriguez-Nieva, K. Agarwal, K. Watanabe, T. Taniguchi, E. A. Demler, P. Kim, H. Park *et al.*, Science **364**, 154 (2019).

[43] R. Sahay, S. Hsieh, E. Parsonnet, L. W. Martin, R. Ramesh, N. Y. Yao, and S. Chatterjee, arXiv:2111.09315.

[44] J. Y. Khoo, F. Pientka, P. A. Lee, and I. S. Villadiego, Phys. Rev. B **106**, 115108 (2022).

[45] N. J. McLaughlin, C. Hu, M. Huang, S. Zhang, H. Lu, H. Wang, Y. Tserkovnyak, N. Ni, and C. R. Du, Nano Lett. **22**, 5810 (2022).

[46] The other components of the magnetic field induce depolarization on the spin, which can be accounted for independently by the aforementioned T_1 spectroscopy [27].

[47] Note that for generalized echo sequences, i.e., CPMG [48], the total duration τ is given by the number of pulses N_p multiplied by the interpulse spacing, τ_p [27].

[48] H. Y. Carr and E. M. Purcell, Phys. Rev. **94**, 630 (1954).

[49] B. I. Halperin and P. C. Hohenberg, Phys. Rev. **177**, 952 (1969).

[50] B. I. Halperin, P. C. Hohenberg, and S.-k. Ma, Phys. Rev. B **10**, 139 (1974).

[51] B. I. Halperin, P. C. Hohenberg, and S.-k. Ma, Phys. Rev. B **13**, 4119 (1976).

[52] Specifically, $S^{zz}(\omega, \mathbf{q})$ can be written as a single parameter scaling function of $\omega/|\mathbf{q}|^z$ with $z = 2$ at the critical point.

[53] E. J. Davis, B. Ye, F. Machado *et al.*, Nat. Phys. **19**, 836 (2023).

[54] Bo L. Dwyer, Lila V. H. Rodgers, Elana K. Urbach *et al.*, PRX Quantum **3**, 040328 (2022).

[55] S. Chakravarty, B. I. Halperin, and D. R. Nelson, Phys. Rev. Lett. **60**, 1057 (1988).

[56] S. Chakravarty, B. I. Halperin, and D. R. Nelson, Phys. Rev. B **39**, 2344 (1989).

[57] S. Tyc, B. I. Halperin, and S. Chakravarty, Phys. Rev. Lett. **62**, 835 (1989).

[58] A. V. Chubukov, S. Sachdev, and J. Ye, Phys. Rev. B **49**, 11919 (1994).

[59] S. Sachdev and J. Ye, Phys. Rev. Lett. **69**, 2411 (1992).

[60] L. M. Norris, G. A. Paz-Silva, and L. Viola, Phys. Rev. Lett. **116**, 150503 (2016).

[61] G. A. Álvarez and D. Suter, Phys. Rev. Lett. **107**, 230501 (2011).

[62] Y. Sung, F. Beaudoin, L. M. Norris, F. Yan, D. K. Kim, J. Y. Qiu, U. von Lüpke, J. L. Yoder, T. P. Orlando, S. Gustavsson *et al.*, Nat. Commun. **10**, 1 (2019).

[63] K. Binder, *Phase Transitions and Critical Phenomena* (Academic Press, New York, 1983), Vol. 8, p 1–444.

[64] J. Cardy, *Scaling and Renormalization in Statistical Physics* (Cambridge University Press, Cambridge, England, 1996), Vol. 5.

[65] S. Hsieh, P. Bhattacharyya, C. Zu, T. Mittiga, T. Smart, F. Machado, B. Kobrin, T. Höhn, N. Rui, M. Kamrani *et al.*, Science **366**, 1349 (2019).

[66] L. W. Martin and A. M. Rappe, Nat. Rev. Mater. **2**, 16087 (2016).

[67] K. Müller and W. Berlinger, Phys. Rev. Lett. **26**, 13 (1971).

[68] R. Bianco, I. Errea, L. Paulatto, M. Calandra, and F. Mauri, Phys. Rev. B **96**, 014111 (2017).

[69] T. Kaneko, T. Toriyama, T. Konishi, and Y. Ohta, Phys. Rev. B **87**, 035121 (2013).

[70] R. J. Elliott, in *Magnetic Phase Transitions*, edited by M. Ausloos and R. J. Elliott, *Magnetic Phase Transitions* (Springer Berlin Heidelberg, Berlin, Heidelberg, 1983), pp. 2–24, ISBN 978-3-642-82138-7.

[71] M. Brando, D. Belitz, F. M. Grosche, and T. R. Kirkpatrick, Rev. Mod. Phys. **88**, 025006 (2016).

[72] S. Ghosh, F. Kargar, A. Mohammadzadeh, S. Rumyantsev, and A. A. Balandin, Adv. Electron. Mater. **7**, 2100408 (2021).

[73] K. Y. Yip, K. O. Ho, K. Y. Yu, Y. Chen, W. Zhang, S. Kasahara, Y. Mizukami, T. Shibauchi, Y. Matsuda, S. K. Goh *et al.*, Science **366**, 1355 (2019).

[74] S. E. Lillie, D. A. Broadway, N. Dontschuk, S. C. Scholten, B. C. Johnson, S. Wolf, S. Rachel, L. C. L. Hollenberg, and J.-P. Tetienne, Nano Lett. **20**, 1855 (2020).

[75] M. Kianinia, S. White, J. E. Fröch, C. Bradac, and I. Aharonovich, ACS Photonics **7**, 2147 (2020).

[76] A. Gottscholl, M. Kianinia, V. Soltamov, S. Orlinskii, G. Mamin, C. Bradac, C. Kasper, K. Krambrock, A. Sperlich, M. Toth *et al.*, Nat. Mater. **19**, 540 (2020).

[77] A. J. Healey, S. C. Scholten, T. Yang, J. A. Scott, G. J. Abrahams, I. O. Robertson, X. F. Hou, Y. F. Guo, S. Rahman, Y. Lu *et al.*, arXiv:2112.03488.

[78] M. Huang, J. Zhou, D. Chen, H. Lu, N. J. McLaughlin, S. Li, M. Alghamdi, D. Djugba, J. Shi, H. Wang *et al.*, Nat. Commun. **13**, 5369 (2022).

[79] L. Rondin, J.-P. Tetienne, T. Hingant, J.-F. Roch, P. Maletinsky, and V. Jacques, Rep. Prog. Phys. **77**, 056503 (2014).

[80] R. Schirhagl, K. Chang, M. Loretz, and C. L. Degen, Annu. Rev. Phys. Chem. **65**, 83 (2014).

[81] F. Casola, T. van der Sar, and A. Yacoby, Nat. Rev. Mater. **3**, 1 (2018).

[82] M. S. Grinolds, S. Hong, P. Maletinsky, L. Luan, M. D. Lukin, R. L. Walsworth, and A. Yacoby, Nat. Phys. **9**, 215 (2013).

[83] M. Pelliccione, A. Jenkins, P. Ovartchaiyapong, C. Reetz, E. Emmanouilidou, N. Ni, and A. C. Bleszynski Jayich, Nat. Nanotechnol. **11**, 700 (2016).

[84] L. Thiel, Z. Wang, M. A. Tschudin, D. Rohner, I. Gutiérrez-Lezama, N. Ubrig, M. Gibertini, E. Giannini, A. F. Morpurgo, and P. Maletinsky, Science **364**, 973 (2019).

[85] U. Vool, A. Hamo, G. Varnavides, Y. Wang, T. X. Zhou, N. Kumar, Y. Dovzhenko, Z. Qiu, C. A. C. Garcia, A. T. Pierce *et al.*, Nat. Phys. **17**, 1216 (2021).

[86] J. R. Maze, A. Gali, E. Togan, Y. Chu, A. Trifonov, E. Kaxiras, and M. D. Lukin, New J. Phys. **13**, 025025 (2011).

[87] M. W. Doherty, N. B. Manson, P. Delaney, F. Jelezko, J. Wrachtrup, and L. C. Hollenberg, Phys. Rep. **528**, 1 (2013).

[88] S. Hong, M. S. Grinolds, L. M. Pham, D. Le Sage, L. Luan, R. L. Walsworth, and A. Yacoby, MRS Bull. **38**, 155 (2013).

[89] T. Mittiga, S. Hsieh, C. Zu, B. Kobrin, F. Machado, P. Bhattacharyya, N. Z. Rui, A. Jarmola, S. Choi, D. Budker *et al.*, Phys. Rev. Lett. **121**, 246402 (2018).

[90] E. Bauch, S. Singh, J. Lee, C. A. Hart, J. M. Schloss, M. J. Turner, J. F. Barry, L. M. Pham, N. Bar-Gill, S. F. Yelin *et al.*, Phys. Rev. B **102**, 134210 (2020).

[91] M. A. McGuire, H. Dixit, V. R. Cooper, and B. C. Sales, Chem. Mater. **27**, 612 (2015).

[92] C. Gong, L. Li, Z. Li, H. Ji, A. Stern, Y. Xia, T. Cao, W. Bao, C. Wang, Y. Wang *et al.*, Nature (London) **546**, 265 (2017).

[93] B. Huang, G. Clark, E. Navarro-Moratalla, D. R. Klein, R. Cheng, K. L. Seyler, D. Zhong, E. Schmidgall, M. A. McGuire, D. H. Cobden *et al.*, Nature (London) **546**, 270 (2017).

[94] J. L. Lado and J. Fernández-Rossier, 2D Mater. **4**, 035002 (2017).

[95] Y. Liu, L. Wu, X. Tong, J. Li, J. Tao, Y. Zhu, and C. Petrovic, Sci. Rep. **9**, 1 (2019).

[96] One important question regards how close to the transition one has to be to observe noise at the MHz scale accessible to our probe: while, in general, this remains an open question, recent work on two-dimensional $CrBr_3$ suggests that there can be a wide parameter regime where slow modes persist due to critical slowing down around the transition point [97].

[97] C. Jin, Z. Tao, K. Kang, K. Watanabe, T. Taniguchi, K. F. Mak, and J. Shan, Nat. Mater. **19**, 1290 (2020).

[98] S. Sangtawesin, B. L. Dwyer, S. Srinivasan, J. J. Allred, L. V. H. Rodgers, K. De Greve, A. Stacey, N. Dontschuk, K. M. O'Donnell, D. Hu *et al.*, Phys. Rev. X **9**, 031052 (2019).

[99] E. Y. Andrei, D. K. Efetov, P. Jarillo-Herrero, A. H. MacDonald, K. F. Mak, T. Senthil, E. Tutuc, A. Yazdani, and A. F. Young, Nat. Rev. Mater. **6**, 201 (2021).

[100] K. F. Mak and J. Shan, Nat. Nanotechnol. 17, 686 (2022).

[101] A. Kreisel, P. J. Hirschfeld, and B. M. Andersen, Symmetry **12**, 1402 (2020).

[102] D.-H. Lee, Annu. Rev. Condens. Matter Phys. **9**, 261 (2018).

[103] Z. Wu, J. Yu, and S. Yuan, Phys. Chem. Chem. Phys. **21**, 7750 (2019).

[104] M. Lesik, T. Plisson, L. Toraille, J. Renaud, F. Occelli, M. Schmidt, O. Salord, A. Delobbe, T. Debuisschert, L. Rondin *et al.*, Science **366**, 1359 (2019).

[105] A. J. Healey, S. C. Scholten, T. Yang, J. A. Scott, G. J. Abrahams, I. O. Robertson, X. F. Hou, Y. F. Guo, S. Rahman, Y. Lu *et al.*, Nat. Phys. **19**, 87 (2023).

[106] M. Huang, J. Zhou, D. Chen, H. Lu, N. J. McLaughlin, S. Li, M. Alghamdi, D. Djugba, J. Shi, H. Wang *et al.*, Nat. Commun. **13**, 5369 (2022).

[107] E. Y. Andrei and A. H. MacDonald, Nat. Mater. **19**, 1265 (2020).

[108] A. L. Sharpe, E. J. Fox, A. W. Barnard, J. Finney, K. Watanabe, T. Taniguchi, M. A. Kastner, and D. Goldhaber-Gordon, Science **365**, 605 (2019).

[109] M. Serlin, C. L. Tschirhart, H. Polshyn, Y. Zhang, J. Zhu, K. Watanabe, T. Taniguchi, L. Balents, and A. F. Young, Science **367**, 900 (2020).

[110] N. Bultinck, S. Chatterjee, and M. P. Zaletel, Phys. Rev. Lett. **124**, 166601 (2020).

[111] Y.-H. Zhang, D. Mao, and T. Senthil, Phys. Rev. Res. **1**, 033126 (2019).

[112] N. Bultinck, E. Khalaf, S. Liu, S. Chatterjee, A. Vishwanath, and M. P. Zaletel, Phys. Rev. X **10**, 031034 (2020).

[113] B. Lian, Z.-D. Song, N. Regnault, D. K. Efetov, A. Yazdani, and B. A. Bernevig, Phys. Rev. B **103**, 205414 (2021).

[114] T. Li, S. Jiang, L. Li, Y. Zhang, K. Kang, J. Zhu, K. Watanabe, T. Taniguchi, D. Chowdhury, L. Fu *et al.*, Nature (London) **597**, 350 (2021).

[115] S. Musser, T. Senthil, and D. Chowdhury, Phys. Rev. B **106**, 155145 (2021).